Accepted Manuscript

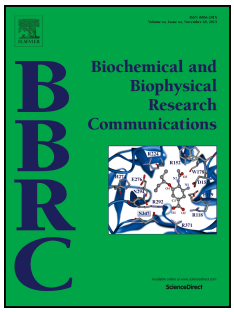

A novel quinazoline-based analog induces G2/M cell cycle arrest and apoptosis in human A549 lung cancer cells *via* a ROS-dependent mechanism

Hailong Shi, Yan Li, Xiaorong Ren, Yaohong Zhang, Zhen Yang, Chenze Qi

PII: S0006-291X(17)30491-6

DOI: 10.1016/j.bbrc.2017.03.034

Reference: YBBRC 37421

To appear in: *Biochemical and Biophysical Research Communications*

Received Date: 23 February 2017

Accepted Date: 11 March 2017

Please cite this article as: H. Shi, Y. Li, X. Ren, Y. Zhang, Z. Yang, C. Qi, A novel quinazoline-based analog induces G2/M cell cycle arrest and apoptosis in human A549 lung cancer cells *via* a ROS-dependent mechanism, *Biochemical and Biophysical Research Communications* (2017), doi: 10.1016/j.bbrc.2017.03.034.

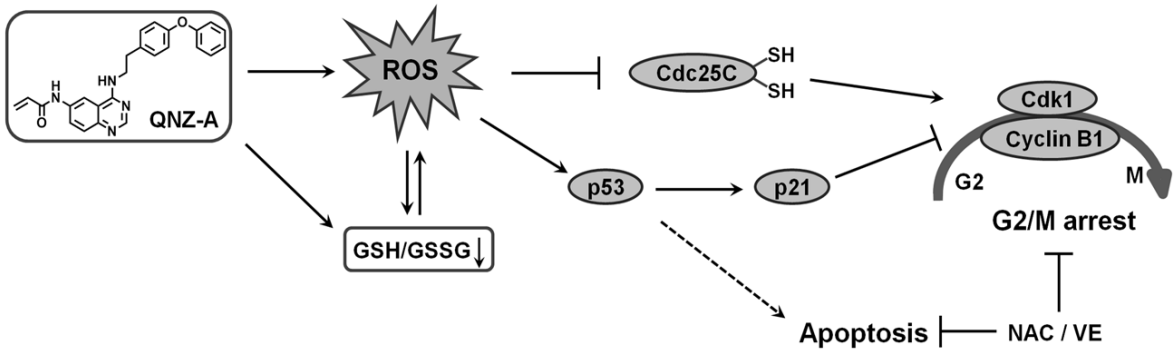

A novel quinazoline-based analog induces G2/M cell cycle arrest and apoptosis in human A549 lung cancer cells *via* a ROS-dependent mechanism

Hailong Shi,[1] Yan Li,[1] Xiaorong Ren, Yaohong Zhang, Zhen Yang, Chenze Qi*

Zhejiang Key Laboratory of Alternative Technologies for Fine Chemicals Process, School of Chemistry and Chemical Engineering, Shaoxing University, Shaoxing, Zhejiang Province 312000, China

*__Corresponding author. Fax:__ +86 575 88345682

E-mail: qichenze@usx.edu.cn

[1] These authors contributed equally to this work.

Abstract

6-amino-4-(4-phenoxyphenylethylamino)quinazoline (**QNZ**) is an excellent quinazoline-containing NF-κB inhibitor also acting as a novel anticancer agent. Considering both the medicinal significance of quinazoline scaffold and the tunable functionality of Michael acceptor-centric pharmacophores in the electrophilicity-based prooxidant strategy, we designed a novel **QNZ**-inspired electrophilic molecule **QNZ-A** by introducing a Michael acceptor unit at position-6 of quinazoline ring in **QNZ**. Our results identified **QNZ-A** as a promising selective cytotoxic agent against A549 cells. **QNZ-A**, by virtue of its Michael acceptor unit, induced reactive oxygen species (ROS) accumulation associated with collapse of the redox buffering system in A549 cells. This caused up-regulation of p53-inducible p21 and down-regulation of redox sensitive Cdc25C along with Cyclin B1/Cdk1, leading to a G2/M cell cycle arrest and final cell apoptosis. By contrast, **QNZ-B**, a reduction product of **QNZ-A** lacking the Michael acceptor unit failed to induce ROS generation and all these cell cycle-related events. In conclusion, this work provided a successful example of designing **QNZ**-directed anticancer agent by a ROS-promoting strategy and identified **QNZ-A** as a selective anticancer agent against A549 cells through G2/M cell cycle arrest and apoptosis *via* a ROS-dependent mechanism.

Keywords: Reactive oxygen species; Cell cycle; G2/M arrest; Michael acceptor; Quinazoline

1. Introduction

Reactive oxygen species (ROS) play important roles in cell growth by regulating the major mediators in many cell signaling pathways [1]. Cells can balance the production of ROS with their removal by an antioxidant defense system under normal physiological conditions [1]. However, once the intracellular redox equilibrium collapses, the excessive ROS may induce direct cellular damage, in turn causing cell growth inhibition and apoptosis by activating specific redox-sensitive cell death signaling pathways [2]. Cancer cells characterized by mitochondrial defects, malignant proliferation and metastatic ability, exhibit greater ROS stress than normal cells, thereby are more susceptible to further ROS production and easier to trigger the critical “toxic threshold” [3, 4]. This intrinsic differences in the redox status between cancer cells and normal cells favors an anticancer strategy that selectively kills cancer cells by ROS-promoting and decreasing the antioxidant capacity of cancer cells, whereas is harmless to the normal cells owing to their lower basal level of endogenous ROS and stronger antioxidant capacity [3, 4].

Numerous promising cytotoxic drugs that kill cancer cells by the abrogation of proliferative signals have been reported to possess ROS-generating ability, including certain commonly used chemotherapeutic agents such as commercial anticancer drug 5-fluorouracil [5] and paclitaxel [6]. One of the most exciting findings regarding ROS-based anticancer agents is that much of these drugs contain electrophilic Michael acceptor pharmacophores which can be employed as tools to fine tune biological activity depending on their multiple reactivities [7]. Michael acceptors can

form covalent adducts with critical thiol residues in redox-sensitive proteins that regulate celluar redox status such as glutathione and thioredoxin, thereby inducing dramatic oxidative stress in target cancer cells [8, 9]. In this respect, for example, natural products parthenolide [10] and piperlongumine [11]characterized by α,β-unsaturated carbonyl moiety in their molecular structures can preferentially induce apoptosis in human cancer cells *via* ROS generation over normal cells, vigorously supporting the concept of ROS-based selective cancer killing [3, 4].

Quinazoline unit has been found as an important scaffold for many drugs with broad spectrum of biological activities such as anti-inflammatory, antioxidant and anticancer [12]. Recent drug optimization efforts have generated several novel quinazoline-derived compounds exerting potent anti-cancer activity *via* ROS generation [13]. In this study, our interest was focused on 6-amino-4-(4-phenoxyphenylethylamino)quinazoline (**QNZ**), a quinazoline-containing compound, known for its excellent NF-κB inhibitory activity [14]. Additionally, **QNZ** also exhibits as a novel anti-cancer reagent [15]. However, the action mechanisms behind are still unclear, and there is as yet scarcely any research related to designing **QNZ**-inspired anticancer agents based on the ROS-promoting strategy. In this study, we tried to design a **QNZ**-based prooxidant by introducing a Michael acceptor unit at position-6 of quinazoline ring in **QNZ** to increase its electrophilicity. To probe the possibility of Michael acceptor-dependent prooxidant mechanism, we synthesized two analogs: **QNZ-A** with a Michael acceptor unit and its reduction product **QNZ-B** lacking the Michael acceptor unit. Our results

confirm for the first time that **QNZ-A** as a novel electrophilic compound can selectively kill human non-small cell lung cancer (A549) cells mainly by ROS-mediated cell cycle arrest and apoptosis. It is worthy of further study for its potentials in the investigation of Michael acceptor-dependent redox intervention related molecular mechanisms and as a possible lead structure to develop new cancer drug.

2. Materials and methods

2.1 Materials

RPMI medium 1640, 3-(4,5-dimethyl-2-thiazolyl)-2,5-diphenyl-2-H-tetrazolium bromide (MTT), Propidium iodide (PI), RNAse, 2',7'-Dichlorofluorescin diacetate (DCFH-DA) were purchased from Sigma-Aldrich (St. Louis, MO, USA). The antibodies against p53, p21, Cyclin B1, Cdk1 and Cdc25C were from Cell Signaling Technology (Beverly, MA, USA). **QNZ**, **QNZ-A** and **QNZ-B** were synthesized in our lab (the details and spectra data shown in the Supplementary Materials).

2.2. Electrophilicity assessment by NMR

^{1}H NMR spectra of **QNZ-A** (50 mM in *d*6-DMSO) before and after the incubation with benzyl mercaptan (75 mM in *d*6-DMSO) at set intervals (3 h, 2 or 5 day) were recorded using a Bruker AV 400 (Bruker Biospin Co. Ltd., Switzerland) spectrometer.

2.3. Cell Culture

A549 cells, human hepatocellular carcinoma (HepG2) cells and human umbilical vein

endothelial (HUVEC) cells (Shanghai Institute of Biochemistry and Cell Biology, Chinese Academy of Sciences) were cultured in RPMI-1640 medium supplemented with 10% (v/v) FBS, 2 g/L $NaHCO_3$, 2 mM glutamine, 100 kU/L penicillin and 100 kU/L streptomycin at 37 °C in an atmosphere of 5% CO_2.

2.4. Cytotoxicity assay

Cells (3×10^3/well) were treated with graded concentrations of test compounds for 48 h, and then incubated with MTT (0.5 mg/mL) for 4 h. When necessary, the cells were pretreated with N-acetylcysteine (NAC, 10 mM), dithiothreitol (DTT, 500 μM) or α-tocopherol (VE, 500 μM) for 1 h before adding **QNZ-A**. Then the medium was substituted with DMSO for OD determination using a microplate reader (Model 550, Bio-Rad, CA).

2.5. Cell cycle and apoptosis analysis

A549 cells (2×10^5 cells/well) were treated with test compounds for 24 h (in cell cycle analysis) or 48 h (in cell apoptosis analysis). When necessary, the cells were pretreated with NAC (10 mM) or VE (500 μM) for 1 h before **QNZ-A** was added. Cells were harvested for cell cycle and apoptosis analysis using a flow cytometer (Becton–Dickinson, San Jose, CA, USA) as described in our previous work [16].

2.6. Intracellular ROS assay

A549 cells (3×10^5 cells/well) treated with test compounds for 4 h or 8 h, with or without pre-incubation with NAC or DTT or VE, were harvested, stained with DCFH-DA and analyzed by flow cytometry (Becton–Dickinson, San Jose, CA, USA)

[17]. The ROS level in HUVEC cells was also assayed after treated with **QNZ-A** (15 μM) for 8h.

2.7. Intracellular glutathione assay

A549 cells (3×10^5 cells/well) treated with compounds as desired were harvested, lysed and centrifugated, the supernatant was used to determine the total glutathione (GSH) and glutathione disulfide (GSSG) levels using a GSH and GSSG Assay Kit (Beyotime Biotechnology, Jiangsu, China) by an Infinite M200 Pro microplate reader (Tecan, USA). The GSH levels were calculated as previously described [17].

2.8. Real-time quantitative PCR (RT-qPCR) analysis

A549 cells (2×10^6 cells/dish) treated with **QNZ-A** (5, 15 μM) for 24 h with or without pre-incubation with NAC were collected and total RNA was extracted using Total RNA Extraction Kit (Tiangen Biotech Co., Ltd., Beijing, China). The reverse transcription was performed at 42 °C for 1 h and 70 °C for 10 min. RT-qPCR was performed using Brilliant II SYBR Green QPCR Master Mix (Agilent technologies, Santa Clara, CA, USA) on a Stratagene Mx3005P QPCR System (Agilent technologies, Santa Clara, CA, USA). The cycling conditions were: 10 min at 95 °C followed by 40 cycles of amplification (30 s at 95 °C and 50 s at 60 °C). All data were analyzed by the ΔΔCt method using GAPDH as the endogenous reference and were normalized to the non-treated control. Primer sequences are shown in Table S1 in Supplementary materials.

2.9. Western Blot analysis

A549 cells (3×10^6 cells/dish) were treated with **QNZ-A** (5, 15 μM) or **QNZ-B** (15 μM) for 24 h with or without pre-incubation with NAC or VE. After cells lysed, the protein lysates were harvested for western blots as previously described [17]. The signals were finally detected using an enhanced ImageQuant chemiluminescence system (GE Healthcare, Pittsburgh, PA, USA).

2.10. Statistical Analysis

Data are expressed as mean ± SD of the results obtained from at least three independent experiments. Significant differences ($P < 0.05$) between the means of two groups were analyzed by Student's t-test using SPSS 17.0 (SPSS Inc., USA).

3. Results

3.1. Synthesis and electrophilicity assay

As is outlined in Fig. 1A, **QNZ-A**, a novel **QNZ** analog, was constructed *via* a nucleophilic acyl substitution reaction between acryloyl chloride and **QNZ**. Its reduction product **QNZ-B**, was obtained by catalytic hydrogenation of **QNZ-A** over Pd/C. To clarify whether introduction of Michael acceptor-pharmacophore could increase the electrophilicity of the parent **QNZ**, the ^{1}H NMR spectroscopy changes of **QNZ-A** in presence of the sulfydryl-containing reagent benzyl mercaptan were monitored. After incubating a mixture of **QNZ-A** and benzyl mercaptan at a molar ratio of 1:1.5 in *d*6-DMSO, the three groups of double doublets of the olefinic protons at δ 5.81, δ 6.31 and δ 6.50 disappeared over time, associating with an appearance of a strong multiplet at δ 2.70 indicative of the conjugate-addition (Fig. 1B). In

comparision, the addition does not occur for **QNZ** and **QNZ-B** under the same conditions (data not shown), implying that **QNZ-A** is more electrophilic by virtue of its Michael acceptor moiety.

3.2. Selective cytotoxicity toward cancer cells in a ROS-dependent fashion

A series of dose-response curves shown in Fig. 1C allowed us to identify **QNZ-A** (IC_{50} = 6.7 μM) as the most excellent anti-proliferative agent in A549 cells. In contrast, its reduction product **QNZ-B** (IC_{50} = 71.1 μM) with the Michael acceptor unit completely abolished, was even less active than the leading **QNZ** (IC_{50} = 41.1 μM), suggesting that introduction of the electrophilic Michael acceptor was essential for enhancing the cytotoxicity. The cytotoxicity of **QNZ-A** against HepG2 cancer cells together with HUVEC normal cells was also tested. Minimal cytotoxicity was observed in HUVEC normal cells, revealing that normal cells display greater tolerance to **QNZ-A** compared to cancer cells, in which A549 cells was the most sensitive one (Fig. 1D). Based on the excellent selectivity, all the further studies on the cytotoxic mechanisms of **QNZ-A** were focused on A549 cells.

Considering ROS as one of the leading causes of growth inhibition and cell death, three antioxidants including NAC, DTT and VE were employed to clarify the role of ROS in the cytotoxicity induced by **QNZ-A**. As shown in Fig. 1E, pretreatment with NAC or DTT, acting as both a ROS scavenger and a sulfhydryl-containing nucleophile to preferentially react with the Michael donor, almost completely reversed the cytotoxicity induced by **QNZ-A**. A significant reversion effect was also achieved for VE as another important ROS scavenger but with no nucleophilic activity. The

194 above results clearly indicate that ROS generation dramatically contributes to the
195 cytotoxicity of **QNZ-A**, and its Michael acceptor unit also plays a pivotal role.

196 **Fig. 1 here**

197 *3.3. ROS-dependent G2/M cell cycle arrest and apoptosis*

198 To investigate the possible mechanisms underlying the cytotoxicity, we further
199 analyzed the effects of **QNZ-A** on cell cycle distribution and apoptosis by flow
200 cytometry. As shown in Fig. 2A, 24 h of treatment with **QNZ-A** caused a remarkable
201 dose-dependent accumulation of cells in G2/M phase. Increasing concentration from 5
202 to 15 μM led to a successive increase of G2/M-phase cell population from 12.57%
203 (control) to 33.69% (15 μM). Additionally, after a longer duration (48 h) treatment,
204 apoptosis of A549 cells was also strikingly triggered by **QNZ-A** in a
205 concentration-dependent manner (Fig. 2B). In contrast, 15 μM of **QNZ-B** exhibited
206 an insignificant effect on both the cell cycle arrest and induction of apoptosis (Fig. 2A
207 and B). In addition, pretreatment with NAC or even VE noticeably reversed the cell
208 cycle arrest and apoptosis induced by **QNZ-A** (Fig. 2A and B), in line with the results
209 obtained by the cytotoxicity assay.

210 **Fig. 2 here**

211 *3.4. ROS accumulation and imbalance of cellular redox homeostasis*

212 Based on the above results, we further measured the intracellular ROS levels in A549
213 cells. As shown in Fig. 3A, treatment with **QNZ-A** caused an obvious intracellular
214 ROS accumulation in a dose- and time-dependent manner. The fluorescence intensity

measured in cells treated with **QNZ-A** (15 μM) were increased by 4.6-fold relative to the vehicle control at 8 h. In contrast, **QNZ-B** had almost no ROS-generating ability under the same conditions. As expected, the ROS accumulation induced by **QNZ-A** was almost completely abolished by pretreating the cells with any one of the antioxidants including NAC, DTT and VE (Fig. 3B). Additionally, compared with the ROS accumulation observed in A549 cells, **QNZ-A** (15 μM) only raised the ROS level by no more than 15% in HUVEC normal cells at 8 h, highlighting a ROS-based cancer cell selectivity.

We subsequently determined the ratio of GSH/GSSG in A549 cells to ascertain whether the ROS accumulation induced by **QNZ-A** resulted in an imbalance of intracellular redox state. After exposed to **QNZ-A** for 4 and 8 h, a dose- and time-dependent decrease and increase for the GSH and GSSG levels in cells was observed, respectively (Fig. 3D and E). Thus the GSH/GSSG ratios calculated based on the measured GSH and GSSG levels were undoubtedly decreased by **QNZ-A** (Fig. 3F). In contrast, **QNZ-B** was inactive in changing the glutathione levels (Fig. 3D-F). And pretreatment with NAC or VE also abolished these alterations induced by **QNZ-A** (Fig. 3D-F), supporting that the falling apart of intracellular redox buffering system was associated with ROS generation.

Fig. 3 here

3.5. Molecular Mechanisms for ROS-Dependent G2/M Cell Cycle Arrest

To further clarify the molecular mechanisms by which **QNZ-A** induced ROS-dependent G2/M cell cycle arrest in A549 cells, the effect of **QNZ-A** on the

redox sensitive G2/M checkpoint regulators was investigated by RT-qPCR and Western blotting (Fig. 4A and B). Upon the treatment with **QNZ-A** (5 or 15 μM) for 24h, an obvious dose-dependent down-regulation of Cdc25C, Cyclin B1 and Cdk1 along with up-regulation of p53 and p21 was observed both on levels of mRNA and protein (Fig. 4A and B). However, Fig. 4B shows that **QNZ-B** (15 μM) barely affected the expression of the above proteins. In addition, pretreatment with NAC or VE reversed all these protein expression changes induced by **QNZ-A** (Fig. 4B), which is in line with the results from the cell cycle analysis, highlighting the pivotal role of ROS in regulating expression of the above redox active cell-cycle-regulatory proteins.

Fig. 4 here

4. Discussion

In this work, **QNZ-A**, a **QNZ** inspired electrophilic molecule, was designed by introducing a Michael acceptor unit (Fig. 1A and B), and was identified as a potential selective anticancer agent in terms of its preferential cytotoxicity toward A549 and HepG2 cancer cells over HUVEC normal cells (Fig. 1D). The cancer cell selectivity was further supported by the significant difference in inducing the accumulation of ROS (Fig. 3C) between A549 and HUVEC cells. Abrogating the cytotoxicity of **QNZ-A** by antioxidants NAC, DTT and VE (Fig. 1E) indicated ROS were involved in the cytotoxicity mechanism. It is worth noting that NAC and DTT acting as both antioxidants and nucleophiles can reverse the cytotoxicity of **QNZ-A** more thoroughly than VE, supporting that Michael acceptor unit also contributes to its activity. In addition, the cytotoxicity of **QNZ-A** towards A549 cells is predominately

mediated by G2/M cell cycle arrest and subsequent apoptosis, in which the Michael acceptor-dependent ROS generation also plays a central role (Fig. 2A and B). This is further supported by the fact that NAC and VE completely block the ROS accumulation induced by **QNZ-A**, while **QNZ-B** as a reduction product of **QNZ-A** with no Michael acceptor-pharmacophore is inactive in inducing ROS-generation (Fig. 3A and B).

The decrease in the intracellular GSH/GSSG ratio induced by **QNZ-A** in A549 cells indicates the collapse of intracellular redox buffering system. However, it is hard to draw firm conclusion about whether the ROS accumulation is the trigger of this change. **QNZ-A** which has proven to be an electrophile reactive to sulfydryl-containing molecules (Fig. 1B), may react directly with millimolar concentrations of intracellular GSH in all probability, causing the decrease of GSH/GSSG ratio. From another standpoint, despite the slight decrease of the GSH levels in A549 cells, the alteration is much more obviously in the GSSG levels than in the GSH levels (Fig. 3D and E), indicating that the decline of GSH/GSSG ratio is more dependent on the dramatic increase of intracellular GSSG levels. In addition, pretreatment with antioxidant VE reversed all the alterations of intracellular GSH, GSSG and GSH/GSSG ratio induced by **QNZ-A** (Fig. 3D-F), reflecting that ROS do contribute to the collapse of redox homeostasis. It can be inferred from the above results that the ROS accumulation would act as both a trigger and an effector of the drop in GSH levels, leading to a vicious cycle and ensuing redox imbalance in A549 cells.

In further research, we investigated the underlying molecular mechanisms for the ROS-dependent G2/M-phase arrest induced by **QNZ-A**. An extensive number of reports focused on redox regulation of cell growth and death, support the view that ROS as key signaling intermediates participate in cell-cycle progression [18-20]. The accumulation of ROS disturb the redox control of cell cycle progression *via* phosphorylation and ubiquitination of cell cycle regulatory proteins such as cyclins, Cdks and Cdk inhibitors, leading to aberrant cell proliferation and apoptosis [18-20]. Our results revealed that the mRNA and protein expression levels of G2/M checkpoint regulators Cyclin B1 and Cdk1 were down-regulated by **QNZ-A** in a ROS-dependent manner in A549 cells (Fig. 4A and B). The Cyclin B1/Cdk1 complex can be activated by a redox sensitive cell-cycle-regulatory protein Cdc25C phosphatase through phosphorylation of Thr161 and dephosphorylation of pThr14 and pTyr15 on Cdk1 [21]. What coincides is that a down-regulation of Cdc25C expression was also observed in A549 cells treated with **QNZ-A** dose-dependently (Fig. 4A and B). In addition, this down-regulation can be rescued by ROS-scavenger (Fig. 4A and B), which is supported by the reported hypothesis that ROS can inactivate Cdc25C through oxidization of cysteine 330 and 377 at the enzyme active site to form intramolecular disulfide [21]. On the other hand, the activation of Cyclin B1/Cdk1 complex is also negatively regulated by p21, a downstream mediator of the tumor suppressor p53 in a stressed situation [22, 23]. Our results showed that **QNZ-A** increased both the mRNA and protein expression levels of p53 and p21 in a ROS-dependent manner (Fig. 4A and B). It is well established that p53 is an important

sensor of cellular stress conditions (such as excess ROS), playing important roles in cell cycle arrest through up-regulating p21 and in apoptosis [22, 23]. So the up-regulation of p53 may contribute not only to the G2/M phase arrest but also the apoptosis induced by **QNZ-A** in A549 cells. **QNZ-B**, by contrast, failed to affect expression of the above redox-sensitive target proteins under the same conditions (Fig. 4B), clearly indicating that electrophilic (Michael acceptor) moiety also at least partially contributes to the collapse the cell-cycle-regulatory system in A549 cells.

In summary, a novel **QNZ** analog, **QNZ-A**, was first identified as a selective cytotoxic agent toward cancer cells *via* a Michael acceptor-dependent prooxidant mechanism. A possible model depicting the actions of **QNZ-A** is presented in Fig. 4C. **QNZ-A**, by virtue of its Michael acceptor unit, can induce ROS accumulation associated with the collapse of the redox buffering system. The ROS burst triggers redox-sensitive signaling pathways: up-regulation of p53 and p21, and down-regulation of Cdc25C and Cyclin B1/Cdk1, leading to a final G2/M cell cycle arrest and apoptosis in A549 cells. The above results represent a clear advantage of **QNZ-A** as a lead compound for ROS-based cancer therapeutic purposes.

Acknowledgements

This work was supported by Zhejiang Provincial Natural Science Foundation of China (Grant No. LQ16C050001), Zhejiang Provincial Natural Science Foundation of China (Grant No. LQ16H090004) and National Natural Science Foundation of China (Grant No. 21302129).

References

[1] A. Bindoli, M. P. Rigobello, Principles in redox signaling: from chemistry to functional significance. Antioxid. Redox Signal. 18 (2013) 1557-1593.

[2] T. M. Buttke, P. A. Sandstrom, Redox regulation of programmed cell death in lymphocytes. Free radical res. 22 (1995) 389-397.

[3] S. C. Gupta, D. Hevia, S. Patchva, B. Park, W. Koh, B. B. Aggarwal, Upsides and downsides of reactive oxygen species for cancer: The roles of reactive oxygen species in tumorigenesis, prevention, and therapy. Antioxid. Redox Signal. 16 (2012) 1295-1322.

[4] L. L. Policastro, I. L. Ibañez, C. Notcovich, H. A. Duran, O. L. Podhajcer, The tumor microenvironment: characterization, redox considerations, and novel approaches for reactive oxygen species-targeted gene therapy. Antioxid. Redox Signal. 19 (2013) 854-895.

[5] S. Afzal, S. A. Jensen, J. B. Sorensen, T. Henriksen, A. Weimann, H. E. Poulsen, Oxidative damage to guanine nucleosides following combination chemotherapy with 5-fluorouracil and oxaliplatin. Cancer Chemother. Pharmacol. 69 (2012) 301-307.

[6] J. Alexandre, Y. Hu, W. Lu, H. Pelicano, P. Huang, Novel action of paclitaxel against cancer cells: bystander effect mediated by reactive oxygen species. Cancer Res. 67 (2007) 3512–3517.

[7] S. Amslinger, The tunable functionality of α,β-unsaturated carbonyl compounds enables their differential application in biological systems. ChemMedChem 5

(2010) 351-356.

[8] F.-F. Gan, K. K. Kaminska, H. Yang, C.-Y. Liew, P.-C. Leow, C.-L. So, L. N. L. Tu, A. Roy, C.-W. Yap, T.-S. Kang, W.-K. Chui, E.-H. Chew, Identification of Michael acceptor-centric pharmacophores with substituents that yield strong thioredoxin reductase inhibitory character correlated to antiproliferative activity. Antioxid. Redox Signal. 19 (2013) 1149-1165.

[9] S. Jayakumar, R. S. Patwardhan, D. Pal, D. Sharma, S. K. Sandur, Dimethoxycurcumin, a metabolically stable analogue of curcumin enhances the radiosensitivity of cancer cells: Possible involvement of ROS and thioredoxin reductase. Biochem. Biophys. Res. Commun. 478 (2016) 446-454.

[10] Y Sun, D. K. St. Clair, Y. Xu, P. A. Crooks, W. H. St. Clair, A NADPH oxidase-dependent redox signaling pathway mediates the selective radiosensitization effect of parthenolide in prostate cancer cells. Cancer Res. 70 (2010) 2880-2890.

[11] L. Raj, T. Ide, A. U. Gurkar, M. Foley, M. Schenone, X. Li, N. J. Tolliday, T. R. Golub, S. A. Carr, A. F. Shamji, A. M. Stern, A. Mandinova, S. L. Schreiber, S. W. Lee, Selective killing of cancer cells by a small molecule targeting the stress response to ROS. Nature 475 (2011) 231-234.

[12] A. Vijaychand, S. N. Manjula, E. N. Bharath, B. Divya, Medicinal and biological significance of quinazoline: A highly important scaffold for drug discovery: A review. Int. J. Pharma. Bio. Sci. 2 (2011) 780-809.

[13] D. Pathania, M. Sechi, M. Palomba, V. Sanna, F. Berrettini, A. Sias, L. Taheri, N.

Neamati, Design and discovery of novel quinazolinedione-based redox modulators as therapies for pancreatic cancer. Biochim. Biophys. Acta 1840 (2014) 332-343.

[14] M. Tobe, Y. Isobe, H. Tomizawa, T. Nagasaki, H. Takahashi, T. Fukazawa, H. Hayashi, Discovery of quinazolines as a novel structural class of potent inhibitors of NF-κB activation. Bioorg. Med. Chem. 11 (2003) 383-391.

[15] F.-H. Wu, Y. Yuan, D. Li, S.-J. Liao, B. Yan, J.-J. Wei, Y.-H. Zhou, J.-H. Zhu, G.-M. Zhang, Z.-H. Feng, Extracellular HSPA1A promotes the growth of hepatocarcinoma by augmenting tumor cell proliferation and apoptosis-resistance. Cancer Lett. 317 (2012) 157-164.

[16] F. Dai, G.-Y. Liu, Y. Li, W.-J.Yan, Q. Wang, J. Yang, D.-L. Lu, D.-J. Ding, D. Lin, B. Zhou, Insights into the importance of exploiting ROS-promoting signaling for designing curcumin-inspired anticancer agents by the case of diarylpentanoids. Free Radic. Biol. Med. 85 (2015) 127-137.

[17] Y. Li, L.-P. Zhang, F. Dai, W.-J. Yan, H.-B. Wang, Z.-S. Tu, B. Zhou, Hexamethoxylated monocarbonyl analogues of curcumin cause G2/M cell cycle arrest in NCI-H460 cells via Michael acceptor-dependent redox intervention. J. Agric. Food Chem. 63 (2015) 7731-7742.

[18] E. H. Verbon, J. A. Post, J. Boonstra, The influence of reactive oxygen species on cell cycle progression in mammalian cells. Gene 511 (2012) 1-6.

[19] E. H. Sarsour, M. G. Kumar, L. Chaudhuri, A. L. Kalen, P. C. Goswami, Redox control of the cell cycle in health and disease. Antioxid. Redox Signal. 11 (2009)

2985-3011.

[20] S. G. Menon, P. C. Goswami, A redox cycle within the cell cycle: ring in the old with the new. Oncogene 26 (2007) 1101-1109.

[21] J. Rudolph, Redox regulation of the cdc25 phosphatases. Antioxid. Redox Signal. 7 (2005) 761-767.

[22] Y. W. Chung, D. Jeong, J. Y. Won, E.-J. Choi, Y. H. Choi, I. Y. Kima, H_2O_2-induced AP-1 activation and its effect on $p21^{WAF1/CIP1}$-mediated G2/M arrest in a p53-deficient human lung cancer cell. Biochem. Biophys. Res. Commun. 293 (2002) 1248-1253.

[23] M. A. O'Reilly, Redox activation of p21Cip1/WAF1/Sdi1: A multifunctional regulator of cell survival and death. Antioxid. Redox Signal. 7 (2005) 108-118.

Figure Legends

Fig.1. Synthesis, electrophilicity and cytotoxicity of **QNZ** analogs. (A) Synthetic route of **QNZ** and its analogs **QNZ-A** and **QNZ-B**. (B) ^{1}H NMR spectra of **QNZ-A** in *d*6-DMSO before and after adding benzyl mercaptan. (C) Cytotoxicity of **QNZ** and its analogs **QNZ-A** and **QNZ-B** against A549 cells. (D) Cytotoxicity of **QNZ-A** against A549, HepG2 and HUVEC cells. (E) Cytotoxicity of **QNZ-A** against A549 cells in the absence or presence of pretreatment with NAC, DTT or VE.

Fig.2. ROS-dependent G2/M cell cycle arrest (A) and apoptosis (B) induced by **QNZ-A** in A549 cells. Cells were treated with the test compounds with indicated concentrations for 24 h (in cell cycle analysis) or 48 h (in cell apoptosis analysis) in the absence or presence of pretreatment with NAC or VE. Data are representative of three independent experiments.

Fig. 3. ROS accumulation and imbalance of cellular redox homeostasis induced by **QNZ-A**. (A) Fold change of ROS stimulated by **QNZ-A** and **QNZ-B** with the indicated concentrations after 4 h or 8 h of treatment in A549 cells. (B) Effect of ROS scavengers NAC, DTT or VE on the ROS accumulation induced by **QNZ-A** in A549 cells. (C) A comparison of ROS accumulation in A549 cells and in HUVEC normal cells treated with **QNZ-A** for 8 h. (D-F) Alterations of GSH levels (D), GSSG levels (E), and GSH/GSSG ratios (F) in A549 cells treated by **QNZ-A** and **QNZ-B** with the indicated concentrations for 4 h or 8 h, and effect of NAC or VE on these alterations. Data are expressed as mean ± SD; n = 3, * P<0.05, ** P<0.01, *** P<0.001, *vs.*

423 control; # P<0.05, ## P<0.01, ###P<0.001.

424 **Fig. 4.** Molecular mechanisms for **QNZ-A**-induced G2/M cell cycle arrest. (A)
425 RT-qPCR analysis of mRNA expression levels of G2/M checkpoint regulators in
426 A549 cells treated with **QNZ-A** for 24 h with or without NAC pretreatment. Data are
427 expressed as mean ± SD; *n* = 3, * P<0.05, ** P<0.01, *** P<0.001, *vs.* control; #
428 P<0.05, ## P<0.01. (B) Western blot analysis of G2/M checkpoint proteins in A549
429 cells treated with **QNZ-A** and **QNZ-B** for 24 h in the absence or presence of
430 pretreatment with NAC or VE. Data are representative of three independent
431 experiments. (B) Proposed mechanisms underlying the ROS-mediated cytotoxicity of
432 **QNZ-A** in A549 cells.

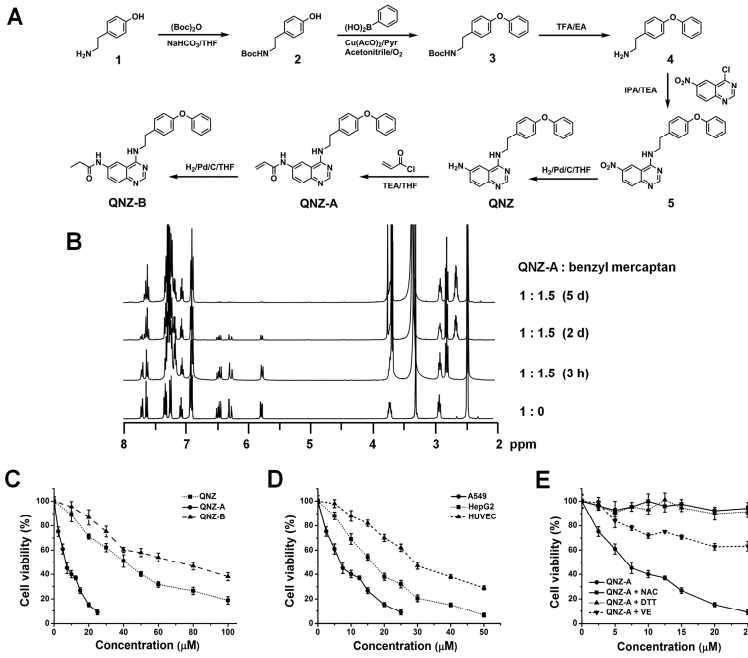

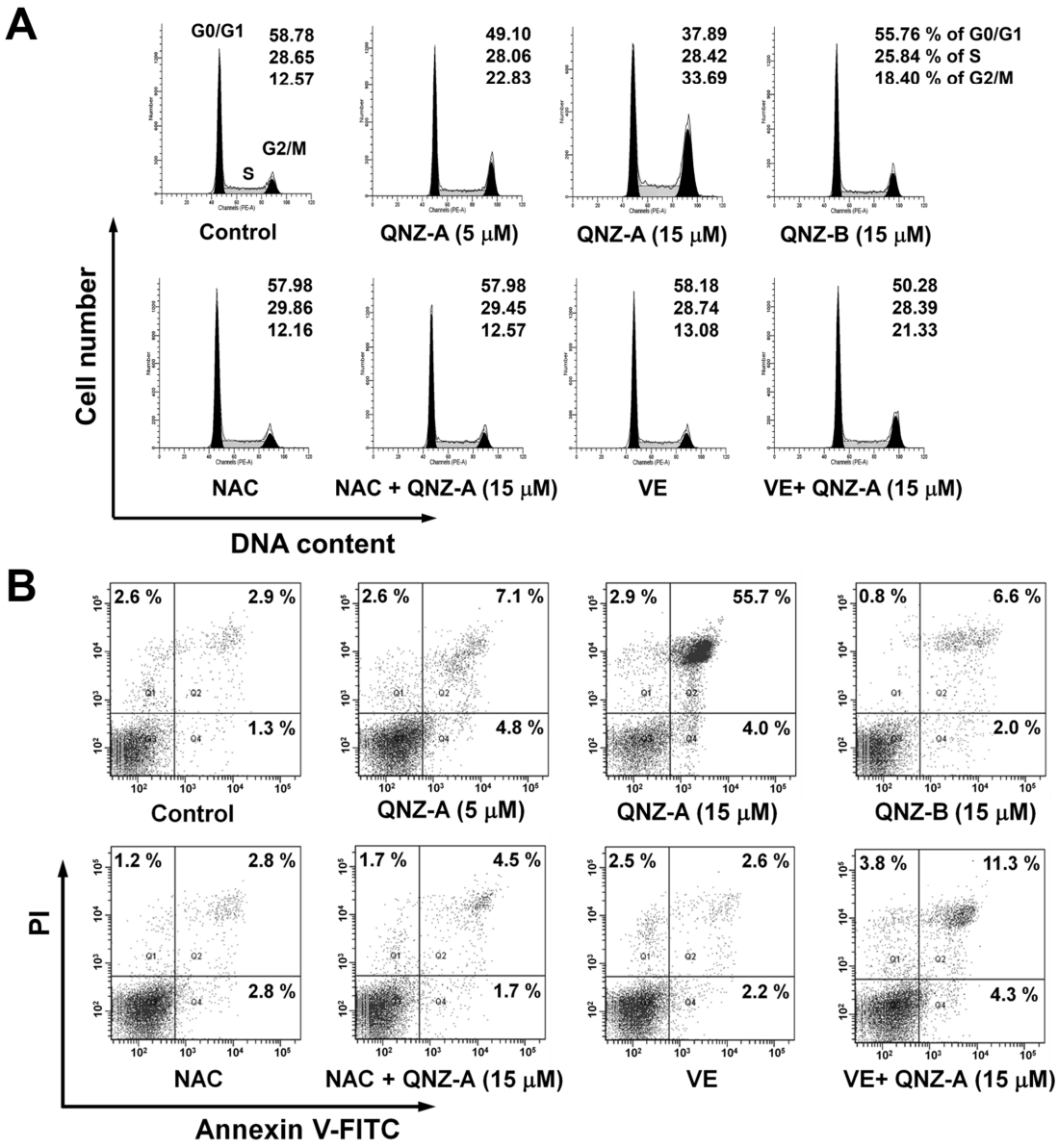
A
G0/G1
58.78
28.65
12.57
G2/M
S
Control
49.10
28.06
22.83
QNZ-A (5 μM)
37.89
28.42
33.69
QNZ-A (15 μM)
55.76 % of G0/G1
25.84 % of S
18.40 % of G2/M
QNZ-B (15 μM)
57.98
29.86
12.16
NAC
57.98
29.45
12.57
NAC + QNZ-A (15 μM)
58.18
28.74
13.08
VE
50.28
28.39
21.33
VE+ QNZ-A (15 μM)
Cell number
DNA content
B
2.6 %
2.9 %
1.3 %
Control
2.6 %
7.1 %
4.8 %
QNZ-A (5 μM)
2.9 %
55.7 %
4.0 %
QNZ-A (15 μM)
0.8 %
6.6 %
2.0 %
QNZ-B (15 μM)
1.2 %
2.8 %
2.8 %
NAC
1.7 %
4.5 %
1.7 %
NAC + QNZ-A (15 μM)
2.5 %
2.6 %
2.2 %
VE
3.8 %
11.3 %
4.3 %
VE+ QNZ-A (15 μM)
PI
Annexin V-FITC

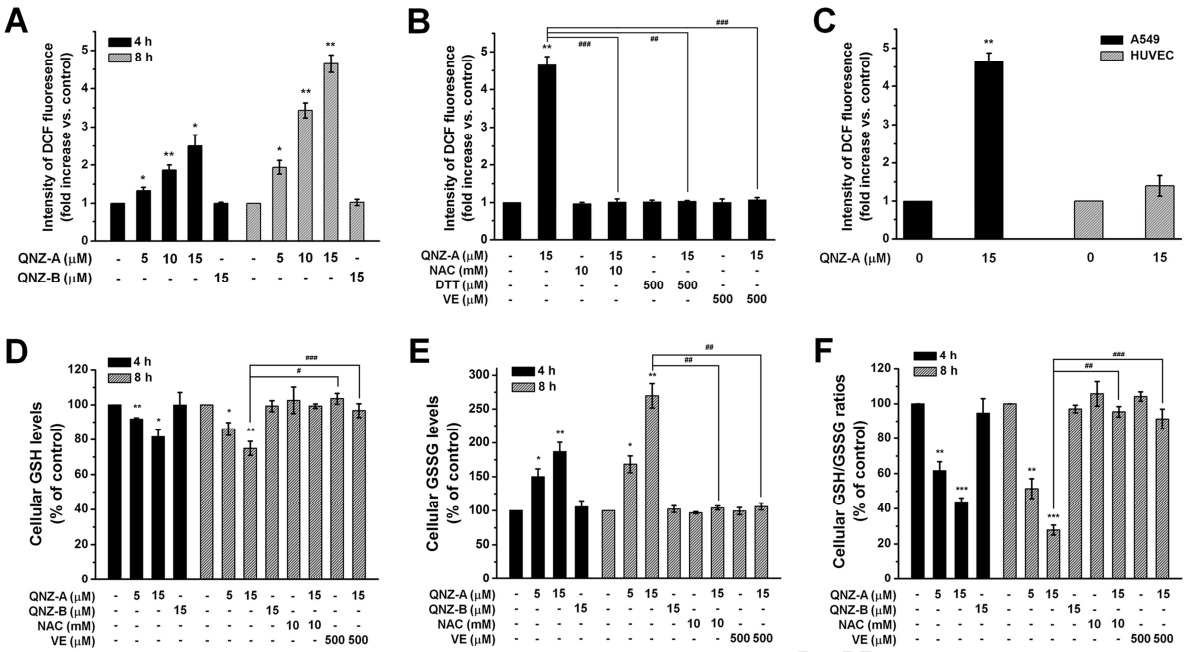

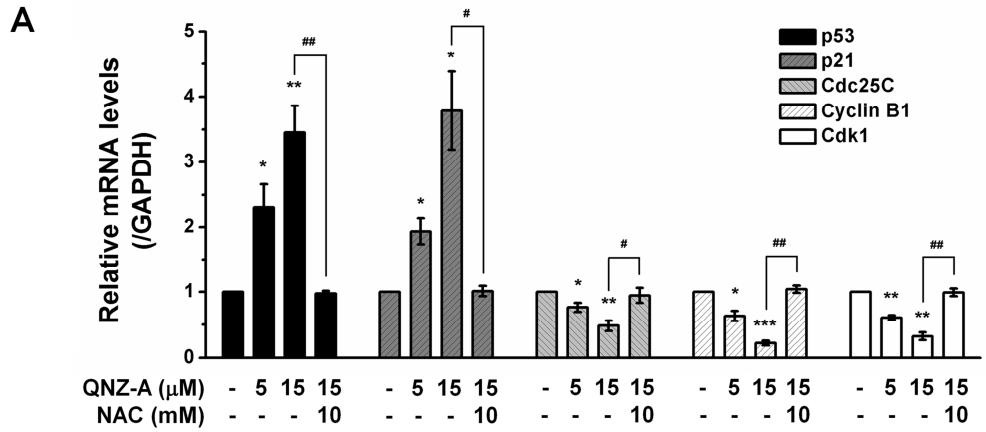

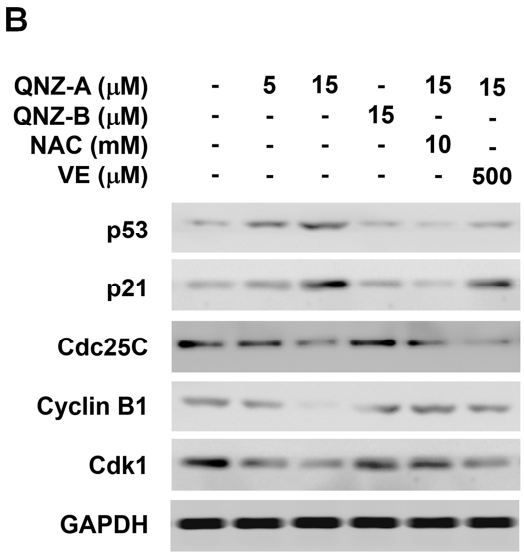

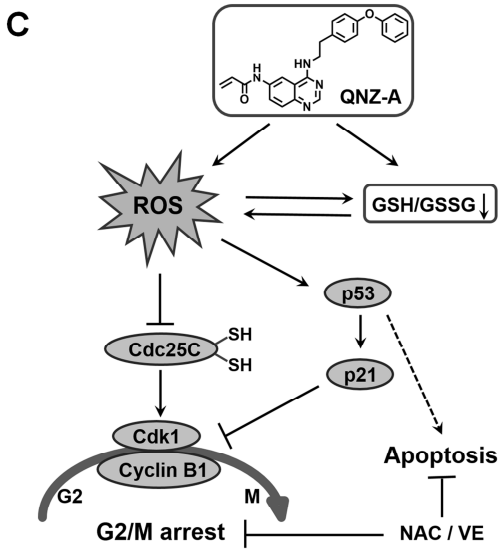

Highlights

- Electrophilic molecule **QNZ-A** selectively kills A549 cancer cells by ROS-promoting.
- The cytotoxic mechanism relies on ROS-dependent G2/M-phase arrest and apoptosis.
- **QNZ-A** up regulates mRNA and protein levels of p53 and p21 in a ROS-dependent way.
- **QNZ-A** induces ROS-dependent G2/M arrest through Cdc25C/cyclin B1/Cdk1 pathway.
- Michael acceptor-dependent prooxidant anticancer strategy is supported.